Chapter 12

Modeling Selective Transport and Desalination in Nanotubes

Michael Thomas, Ben Corry, Shin-Ho Chung, and Tamsyn A. Hilder

CONTENTS

12.1 MOTIVATION FOR MODELING NANOTUBES

At first, it would seem that nanotubes would make unlikely candidates for improving water permeation through membranes. The hydrophobic interior of a carbon nanotube seems a forbidding place for water molecules. Yet, it is this hydrophobic surface that imparts remarkable transport properties onto nanotubes.

The groundbreaking computer modeling work of Hummer et al. predicted that carbon nanotubes would spontaneously fill when immersed in water (Hummer et al. 2001). Using a technique called molecular dynamics (MD), the (6,6) CNT investigated in the study was found to fill with a single chain of hydrogen-bonded water molecules (Figure 12.1). These hydrogen bonds are, on average, longer lasting and more highly oriented than in bulk water, with each water molecule free to rotate about its hydrogen bond axes. This phase of water within the (6,6) nanotube has been described as vapor like and is stabilized through an increase in entropy (compared to bulk water) (Pascal et al. 2011). Ice-like and bulk liquid-like phases are observed in larger-diameter nanotubes.

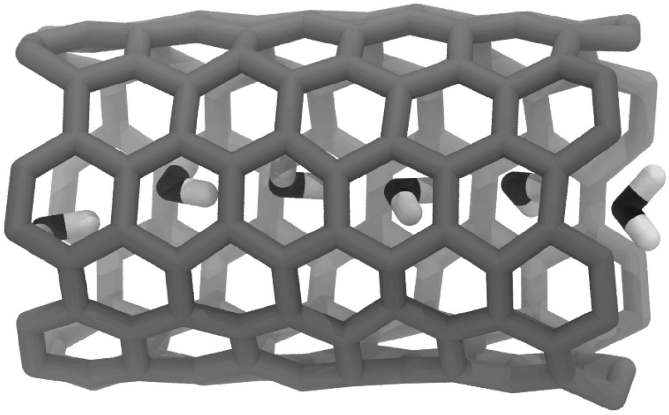

Figure 12.1 Single chain of hydrogen-bonded water molecules in a (6,6) carbon nanotube.

The computer modeling study conducted by Hummer et al. was the first in which the extraordinary rapid transport properties of nanotubes were alluded to. Water was seen to conduct through the nanotube at a similar rate to a biological counterpart, the transmembrane aquaporin-1 channel. Aquaporin allows the passage of water, but not ions and other species, in and out of a cell. Water conduction in the nanotubes occurs in small bursts that are said to flow with very little resistance. Only very small interactions are present between the hydrophobic surface of the nanotubes and the water molecules, resulting in the near-frictionless flow of water.

Landmark experimental studies followed this early modeling work. Aligned nanotube membranes constructed by Hinds et al. (2004) were examined for the gas and ion permeation properties. Although, it was not until Majumder et al. constructed membranes composed of arrays of aligned multiwalled carbon nanotubes with pore diameters of about 7 nm that water permeation was investigated (Majumder et al. 2005). Water flow rates through this membrane were found to be similar to the aquaporin-1 and many orders of magnitude larger than suggested by the Hagen–Poiseuille equation, a conventional continuum flow model. The slip length of these nanotubes was found to be incredibly large, three to four orders of magnitude larger than the pore diameters. These results indicate that the interior of the nanotube offered a near-frictionless surface for the water molecule to flow across, as predicted by computer modeling studies.

Experiments by Holt et al. (2006) demonstrated that these amazing rapid transport properties still occur in narrower nanotubes. Membranes composed of 1.3–2.0 nm diameter carbon nanotubes exhibited water flow rates three orders of magnitude larger than predicted by a continuum model and were consistent with the rates predicted from MD simulations by Hummer et al. Slip lengths were again found to be three to four orders of magnitude larger than the pore diameter, demonstrating that the near-frictionless flow of water also occurs in narrow nanotubes.

Nanotubes also have the ability to reject ions from permeating through the pore, while allowing water to flow. The dipole of the water molecules align to the charge of the ion solvated in bulk water. A monolayer of water molecules becomes bound to the ion, called the solvation shell. In wider nanotubes, ions are able to pass with the full complement of water molecules in their solvation shell. There is insufficient space for this to occur in narrow nanotubes. Some water molecules

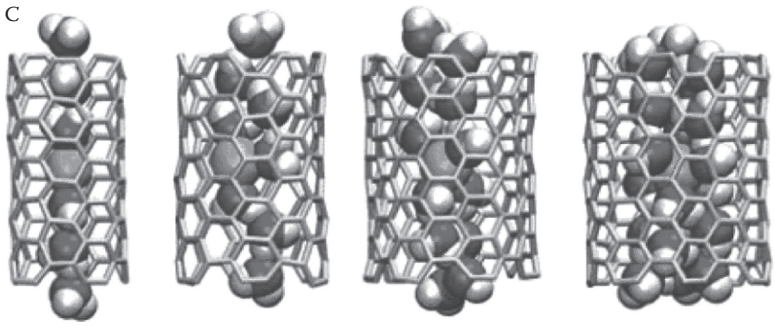

Figure 12.2 In narrow nanotubes (left), very few water molecules coordinate with a permeating ion (sodium). In wider nanotubes (right), water coordination is more bulk like, resulting in a smaller energy barrier for ion conduction. Oxygen is represented in black, hydrogen in white, and carbon in gray. (Reprinted with permission from Corry, B.A., Designing carbon nanotube membranes for efficient water desalination, *J. Phys. Chem. B*, 112(5), 2008, 1427–1434. Copyright 2008 American Chemical Society.)

must be removed from the solvation shell for the ion to fit inside the nanotube, and there is an energetic cost to do this. This makes it far less likely for ions to permeate narrow tubes. Modeling investigations predicted that the rejection of small ionic species, such as Na^+ and Cl^-, could be achieved by hydrophobic pores (Beckstein and Samsom 2004, Dzubiella and Hansen 2005, Corry 2006) and by pristine carbon nanotubes specifically (Peter and Hummer 2005). Ion rejection rates become larger as the nanotube becomes narrower, due to the need to partially desolvate an ion passing through narrow pores (Figure 12.2; Corry 2008).

Ion rejection by nanotubes (shown in Figure 12.3) was demonstrated experimentally by Fornasiero et al. (2008). Nanotubes with pore diameters 1–2 nm were shown to partially reject a number of salts, including Na^+ and Cl^-, with rejection reaching 98% under certain conditions. Nanotubes in this study were made by conformal deposition, followed by chemical etching to remove the caps at the end of the tube. The latter process functionalizes the ends of the nanotubes with carboxylic, carbonyl, and hydroxyl groups. Ion rejection was found to be dependent on pH, indicating that the electrostatic interactions between the ions and the functional groups dominate over steric effects; the desolvation of ions plays little role in salt rejection for nanotubes with pore diameters 1–2 nm. Additionally, the rejection rate was found to decrease as the concentration of the salt increased.

The rapid water transport and ion rejection properties make nanotubes ideal for a number of applications, including environmental sensors, antimicrobial agents, and renewable energy technologies. This chapter will focus on the use of nanotubes in water desalination, an application that pushes the boundaries of these two properties. Water desalination is the process in which seawater or brackish water is taken and progressively treated, removing smaller and smaller particles, until the water is potable. Various methods are employed to remove larger particles at each step. Traditionally, coagulants have been the most popular way of removing larger species by combining small particles into larger particles (Valavala et al. 2011). Other methods are also used, including adsorbents, oxidants, and granular media, depending on the quality of the intake water. More recently, ultrafiltration and microfiltration techniques have become more popular. These methods force water through membranes containing microscopic pores, while larger particles are excluded based on their size.

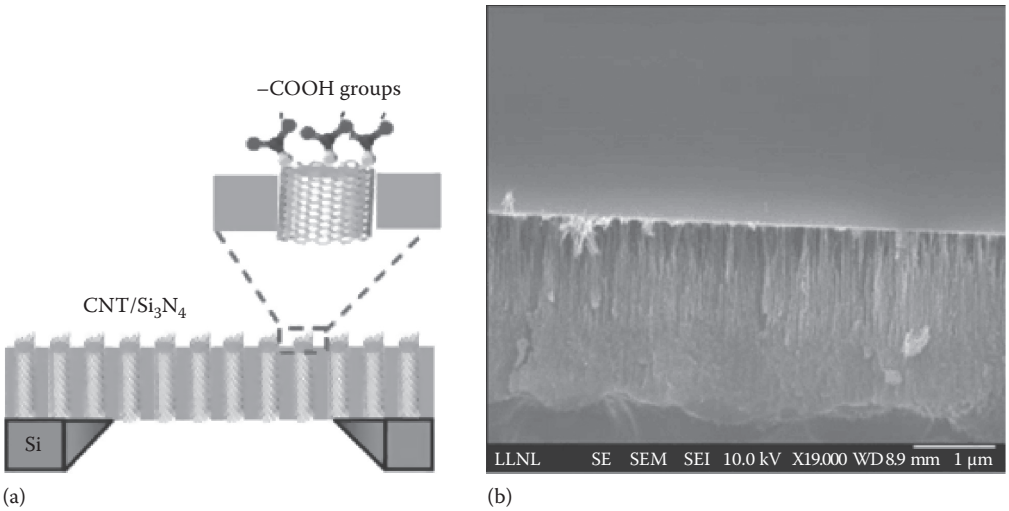

Figure 12.3 (a) A schematic of carbon nanotubes embedded in a silicon carbide matrix. Functionalization of the nanotube ends with carboxylate groups is shown in the inset. (b) A scanning electron image of the cross section of carbon nanotube/silicon nitride matrix. (Reprinted with permission from Fornasiero, F., Park, H.G., Holt, J.K. et al., Ion exclusion by sub-2-nm carbon nanotube pores, *Proc. Natl. Acad. Sci. USA*, 105, 2008, 17250–17255 and Copyright 2008 National Academy of Sciences, U.S.A.)

By far, the most energy-intensive step in the desalination process is the removal of small ionic species, particularly Na^+, K^+, and Cl^-, from water. Currently, the most popular method of removing these species is reverse osmosis filtration where the intake salt solution is placed under a large pressure and forced through a semipermeable membrane. This membrane allows water to permeate, but not ions, producing potable water. More than 95% of the ions must be rejected to produce potable water from typical seawater, although this number will vary depending on the type of input water. A large pressure must be used to overcome the osmotic pressure of the system: the desire for potable water to flow backward through the semipermeable membrane to equalize the salt concentrations. Additional pressure above the osmotic pressure must be applied to achieve usable potable water fluxes.

One measure of the membrane efficiency is the *permeability* of the reverse osmosis membrane, the amount of water flux per unit of force passing through the membrane. The best current reverse osmosis membranes are polyamide-based thin-film composites that can achieve a permeability of 3.5×10^{-12} m^3 m^{-2} Pa^{-1} s^{-1} (m^3 of water per m^2 of membrane per Pascal per second) and sufficient salt rejection. It is thought that nanotube-based desalination membranes may offer a way to increase the membrane permeability, and thus the efficiency of the reverse osmosis process, while maintaining the necessary ion rejection.

Computer modeling is at the forefront of nanotube-based device design, guiding the experimental processes needed to produce benefits to the wider community. Researchers are using a range of modeling techniques to unravel the fundamental concepts underlying transport through nanotubes. Using these results, new-generation technology, such as nanotube-based desalination membranes, can be constructed and implemented. The remainder of this chapter discusses how researchers model nanotubes computationally, as well as the contribution of computational modeling toward our understanding of the water permeation and salt rejection properties of nanotubes.

12.2 MODELING APPROACHES

12.2.1 Molecular Dynamics

Many computational methods have been used to model nanotubes and investigate their various properties: from highly detailed, but computationally intensive, quantum mechanical calculations to the fast, but less detailed, continuum models. MD is a computational method that provides a good balance between detail and speed that is routinely employed to model the dynamics and energetics of systems comprising up to a million atoms.

MD is a method of numerically solving classical equations of motion on a system composed of a number of particles. Atoms are modeled as charged spheres, incorporating the nucleus and electrons into a single particle. In quantum mechanical methods, these are modeled separately, while in continuum models, larger numbers of atoms are modeled as blocks of dielectric material.

A force field is a set of empirically and quantum mechanically derived values used to determine the strength of the interactions between atoms in MD simulations. The force field describes how atoms interact with one another. The ability of MD to produce accurate results depends on the ability of the force field to describe these interactions accurately. Much time and effort is spent developing force fields, many of which have been constructed and optimized for particular types of systems, such as proteins, liquids, and solids. Force fields can be polarizable or nonpolarizable; to include polarization is to account for an atom's change in response to a change in the surrounding electric field. Nonpolarizable force fields, such as CHARMM (MacKerell et al. 1998), Gromos (Scott et al. 1999), and Amber (Salomon-Ferrer et al. 2013), have been the most popular to date, as polarizable force fields require a lot of computing power. However, as computing power increases, the usefulness and popularity of polarizable force fields will also increase.

A force field is composed of parameters that describe a variety of interactions, such as

1. The stretching of bonds
2. The bending of angles
3. The torsion of dihedral angles
4. van der Waals interactions
5. Electrostatic interactions

The stretching, bending, and torsions are known as *bonded interactions*; they define how atoms covalently bonded to one another behave. The van der Waals and electrostatic interactions are known as "nonbonded" interactions as they describe how atoms interact through space. The parameters describing each of these interactions for each combination of atoms must be determined. For example, a bond strength, k, and an equilibrium separation distance, $\boldsymbol{x}_0$, are required to determine the force, $F(\boldsymbol{x}) = \frac{1}{2}k(\boldsymbol{x} - \boldsymbol{x}_0)^2$, of a bond stretch, which models the covalent bonding between atoms. Another example is the charge on each atom to calculate the force due to electrostatic interaction. These parameters are usually determined by high-level quantum calculations and are validated by their ability to replicate bulk properties of the particular molecule being described, such as heat of vaporization, dipole moment, or a variety of spectroscopic properties. These parameters describe only the average properties of a large number of a particular type of molecule, and so in conditions or environments that stray significantly from this, inaccurate results are likely to be produced. For instance, nonpolarizable force fields are unable to handle polarization explicitly; it is accounted for only in an average sense by being incorporated into other parameters.

Before the commencement of an MD simulation, a set of initial coordinates and velocities are required. Coordinates are usually obtained from experimental structure determination techniques, such as X-ray crystallography, or built using one of a number of various molecular visualization programs. Initial velocities are usually randomly assigned from a Maxwell–Boltzmann distribution centered on the desired temperature. Once the coordinates and velocities are assigned, the force acting on each atom in the initial coordinates is calculated using parameters from the force field. Using this force, we can describe how each atom will move over a very small amount of time, called a time step, which is usually 1–2 fs. Once the atoms have moved, the force experienced by each atom is recalculated. This process iterates for a defined number of time steps, creating a time evolution of the system described by the initial coordinates.

MD is an important tool for researchers investigating nanotubes, especially in the context of desalination. The atomic resolution of MD simulations allows for the investigation of many important features over timescales long enough to collect adequate statistics. It allows us to capture many permeation events of single ions and water molecules through nanotubes. Within MD, there are a variety of techniques used to describe particular aspects of nanotube function that other methods cannot offer, either due to insufficient detail or prohibitively long computing times. For example, these techniques can be used to calculate the energetics of ion and water permeation. This allows us to probe nanotubes to understand how their remarkable permeation properties arise and how we may optimize these properties.

MD does not have the ability to model bond formation or destruction as electrons are not modeled explicitly, as in quantum mechanical simulations. This means that MD is unable to capture any chemistry that may take place. This may be of particular importance when considering possible bond formation during chemical fouling of desalination membranes or the role that functional groups attached to the end of nanotubes may play. However, the exclusion of chemistry from MD allows us to conduct simulations over far greater timescales than can be achieved using quantum mechanical calculations.

12.2.2 Modeling Membranes

The pore size and chirality of nanotubes are defined by their chiral vector, $C = n\boldsymbol{a}_1 + m\boldsymbol{a}_2 = (n,m)$, resulting in three general forms: armchair (n,n), chiral (n,m), and zigzag $(n,0)$, as shown in Figure 12.4. The majority of computational studies have focused on the armchair-type nanotube. It is generally assumed that the chirality of the nanotube does not affect transport properties (Alexiadis and Kassinos 2008), although there is some suggestions that it may (Won et al. 2006). Nanotubes are usually constructed using automated nanotube builders, such as the Carbon Nanostructure Builder available in the molecular visualization program VMD (Humphrey et al. 1996), providing the initial coordinates in order to commence an MD simulation.

It must be decided if the nanotube will be embedded in a membrane matrix or not. The matrix is an impermeable material that composes the majority of the membrane, through which nanotubes create pores. Whether or not a matrix should be included will depend on what aspect is to be investigated. Initial investigations by Hummer et al. modeled carbon nanotubes in bulk water in order to investigate their water filling and transport properties (Hummer et al. 2001). Most subsequent investigations have modeled nanotubes embedded in a matrix of some sort. In experiments, nanotubes are often embedded in silicon nitride (Holt et al. 2006) or polystyrene film (Hinds et al. 2004, Majumder et al. 2005) matrices. In MD simulations, nanotubes have been embedded in a variety of matrices including silicon nitride (Hilder et al. 2009, 2009a), lipid bilayers (Hilder 2012), and graphene bilayers (Gong 2010, Su and Guo 2012), as shown in Figure 12.5.

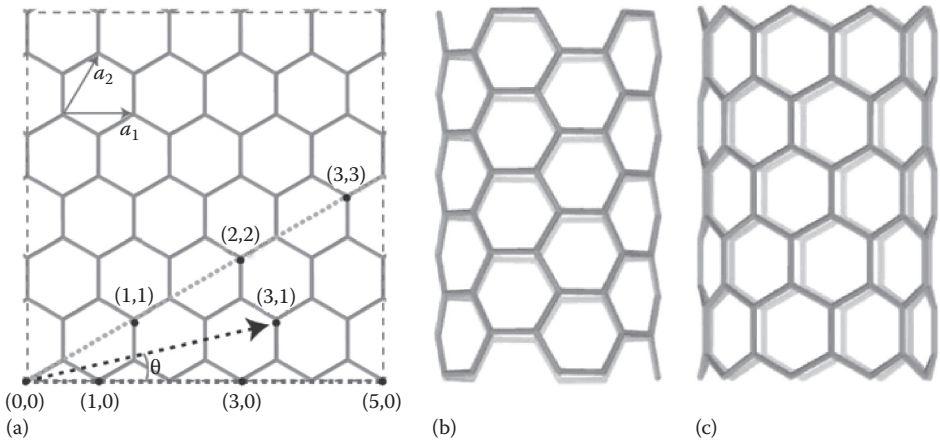

Figure 12.4 (a) Examples of chiral vectors on a graphene sheet. The dashed gray line follows the circumference of an armchair-type tube, the dashed black arrow follows a chiral-type tube, and the dashed horizontal line follows a zigzag-type tube. (b) A (5,5) nanotube, an example of an armchair-type tube. (c) A (9,0) nanotube, an example of a zigzag tube. (Reproduced from Maiti, A., *Nat. Mater.*, 2, 440, 2003.)

This creates a barrier, forcing water and ions to permeate through the nanotube if they are to get from one side to the other. This also means that additional forces can be added to the atoms in the system to model an applied pressure or an electric field in order to determine the water permeation and/or salt rejection properties. In this instance, the atoms composing the nanotube and matrix must be held in place by additional constraints to avoid their translation due to the applied pressure or electric field.

An alternative approach, developed by Zhu and Schulten (2003), uses a membrane constructed solely of nanotubes, rather than embedding the nanotube in a matrix, as shown in Figure 12.5d. By packing the nanotubes close together (e.g., hexagonal packing), there is not enough space for molecules to pass between the nanotubes, and so flow is confined to the interior of the tubes. The atoms of the nanotubes are held in place by artificial constraints, so as to allow a pressure difference to be added to the system without degradation of this membrane. This type of setup is popular as it increases the sampling rates of species permeating the nanotubes as it allows fluxes to be measured across many nanotubes instead of just one. This allows a reduction in the time needed for simulation to achieve the same accuracy in the flux.

Finally, water and salt ions are added to the nanotube/matrix system. Water molecules are usually added to either side of the membrane in a box shape, to which ions can be added. This shape allows for the system to be treated in a periodic fashion; water molecules and ions are able to wrap around from one edge to the other in the x, y, and z directions so that boundary effects do not affect the simulation.

12.2.3 Permeation Properties

It is the water flux and salt rejection properties of nanotubes that we wish to understand for their application as desalination membranes. The water flux of a membrane is the number of water molecules crossing through a given area of membrane in a particular period of time and has units of $m^3\ m^{-2}\ s^{-1}$. Water must be driven across the membrane by some force; this is often a hydrostatic pressure

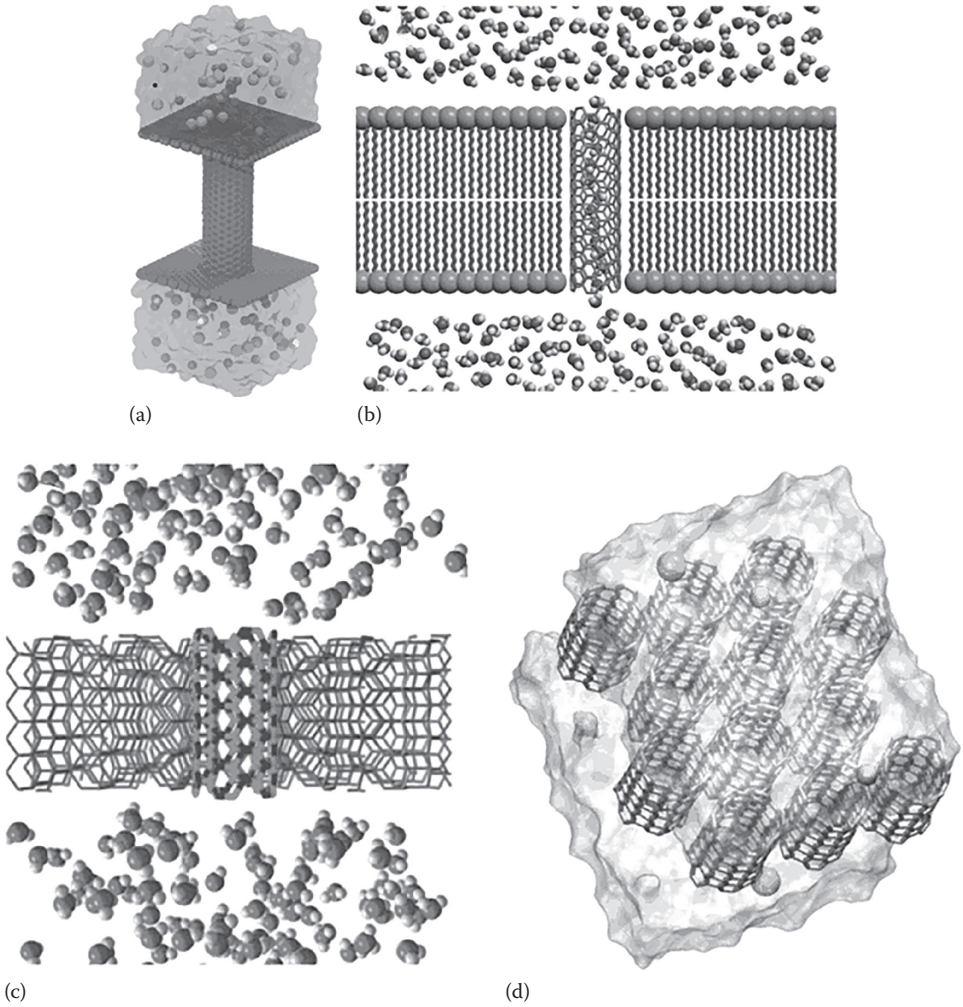

Figure 12.5 Molecular dynamic simulation of nanotubes embedded in various matrices. (a) Graphene bilayers. (b) Lipid bilayers. (Adapted with permission from Hilder, T.A., Yang, R., Gordon, D., Rendell, A.P., and Chung, S.-H., Silicon carbide nanotube as a chloride-selective channel, *J. Phys. Chem. C*, 116(7), 2012, 4465–4470. Copyright 2012 American Chemical Society.) (c) Silicon nitride membrane. (Adapted from Hilder, T.A. et al., *Small*, 5(19), 2183, 2009, image has been rotated and cropped.) (d) Array of nanotubes. (Adapted with permission from Corry, B.A., Designing carbon nanotube membranes for efficient water desalination, *J. Phys. Chem. B*, 112(5), 2008, 1427–1434. Copyright 2008 American Chemical Society.)

(as implemented by Zhu et al. [2002, 2004]) or sometimes an osmotic pressure (Kalra et al. 2003). The hydrostatic or osmotic pressure is quoted along with the water flux values so that comparisons can be made between different modeling investigations. A more explanative, albeit more time consuming, way to represent water permeation is the water permeability of a membrane. This measures how the water flux across the membrane responds to different pressures and is measured in units of $m^3\ m^{-2}\ s^{-1}\ Pa^{-1}$ (water flux per unit pressure). For MD investigations, the units of flux and permeability are often given as molecules $tube^{-1}\ ns^{-1}$ and molecules $tube^{-1}\ ns^{-1}\ MPa^{-1}$, respectively.

Salt rejection measures how good a membrane is at stopping the passage of salt ions. It is expressed as a ratio of the relative amount of permeant ions to the relative amount of permeant water molecules. For instance, the salt rejection is often described by

$$\text{Ion Rejection} = 1 - \frac{n_{\text{permeant ions}} / n_{\text{total ions}}}{n_{\text{permeant water}} / n_{\text{total water}}},$$

where

$n_{\text{permeant ions}}$ is the number of permeant salt ions
$n_{\text{total ions}}$ is the total number of salt ions in the simulation
$n_{\text{permeant water}}$ is the number of permeant water molecules
$n_{\text{total water}}$ is the total number of water molecules

It is usually expressed as a percentage. This definition can also be used for individual ion types to determine if the membrane is better at rejecting some ion types over others. This can be helpful for aiding the design of desalination membranes, as well as for other applications, such as ultra-sensitive biosensors (Hilder et al. 2011).

In order to measure the permeability of a nanotube-based membrane, a water flow through nanotubes must be induced. There are a number of ways this can be achieved, but as desalination facilities use pressure to achieve permeation, this is what is commonly used in MD. To do this, we need to add a pressure difference across the membrane. A hydrostatic pressure can be introduced by adding an additional force to a subset of water molecules during the force calculation step in the MD algorithm. This force acts to drive water molecules across the membrane, but as water flow across the membrane is limited, a high density of water will build up on this side of the membrane. On the other side of the membrane, water will be removed from near the membrane, but not replaced quickly enough, creating a region of low density. These two regions of differing density define the pressure difference. In practice, the force is applied to molecules only far from the membrane such that there is a region of constant density on each side.

Free energy profiles (like those displayed in Figure 12.6) allow us to observe the energetics of water and ion permeation through nanotubes. A useful MD technique for determining these free energy profiles is the potential of mean force (PMF) calculation (Torrie and Valleau 1974). It can be used to explain why water fluxes and salt rejection are different for different nanotubes. A PMF describes how the free energy of a simulation system changes as an atom, or groups of atoms, is moved along a particular reaction coordinate. This can be used, for example, to determine the energetics of an ion or water molecule permeating through a nanotube, as shown in Figure 12.6. Umbrella sampling is a commonly used technique that is used to determine a PMF. A number of simulations are conducted wherein atoms are biased to a particular position along the reaction coordinate in each simulation (in nanotubes, this is usually the radial and axial coordinates through the nanotube), and the value of the reaction coordinate is recorded. The combined set of results are then unbiased, usually using the weighted histogram analysis method (Kumar et al. 1992). This is done to achieve adequate sampling of unlikely configurations along the reaction coordinate to increase the accuracy of the free energy results.

Using these tools, we can now investigate various properties of nanotubes as follows:

- What nanotube dimensions offer the best water flux/permeability while maintaining greater than 95% salt rejection?
- Is water flow in the tube really *near-frictionless*?
- How do functional groups at the nanotube openings affect their function?
- How does the material that the nanotube is composed of (carbon, silicon carbide, boron nitride) affect transport properties?

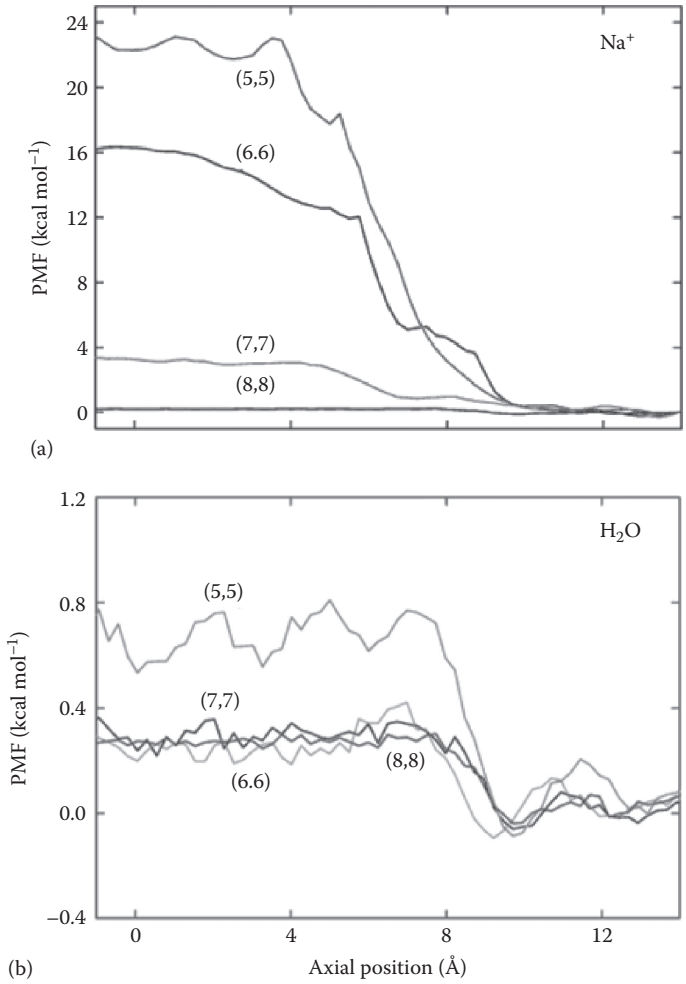

Figure 12.6 An example of a PMF calculation. A PMF of (a) a sodium ion and (b) a water molecule passing through a carbon nanotube. The (5,5) CNT has the smallest pore diameter, and the (8,8) has the largest. (Reprinted with permission from Corry, B.A., Designing carbon nanotube membranes for efficient water desalination, *J. Phys. Chem. B*, 112(5), 2008, 1427–1434. Copyright 2008 American Chemical Society.)

Using MD techniques, researchers have been able to provide answers to these questions. The subsequent section will explore what researchers have learned about nanotubes and their desalination properties through simulation with MD.

12.3 WATER AND ION PERMEATION PROPERTIES OF NANOTUBES

12.3.1 Spontaneous Water Filling

MD simulations of a (6,6), 0.81 nm diameter carbon nanotube immersed in water demonstrated that water molecules will spontaneously enter and remain in the pore (Hummer 2001). In contrast, a (5,5) carbon nanotube (diameter of 0.69 nm) will only partially fill with water

molecules (Won and Aluru 2007) or alternate between empty and filled states (Corry 2008). All nanotubes with larger pore diameters will spontaneously fill. Typically, carbon nanotubes are modeled with a zero partial charge on each carbon atom. In contrast, boron nitride nanotubes and silicon nitride nanotubes have differing partial charges on each boron and nitrogen, and silicon and carbon atoms, respectively. These charges, combined with the van der Waals parameters, allow water molecules to hydrogen-bond with the nitrogen atoms (Won and Aluru 2008). As such, boron nitride tubes spontaneously fill at smaller pore diameters than carbon nanotubes, with the 0.69 nm (5,5) spontaneously filling, owing to the increased van der Waals and electrostatic interactions between the nanotube atoms and the water molecules filling the pore (Won and Aluru 2007, 2008, Hilder et al. 2009). Therefore, it is likely that the filling of silicon carbide nanotubes is similar to the filling of boron nitride nanotubes; water spontaneously enters smaller pore diameters than carbon nanotubes (Yang et al. 2011, Taghavi et al. 2013).

The confinement of water molecules within a nanotube is thermodynamically favorable, that is to say that the free energy is lower in a filled state than an unfilled state (Pascal et al. 2011). However, the driving force differs with the pore diameter:

- Filling is entropy driven in the smaller-diameter (5,5) and (6,6) carbon nanotubes (0.81–1.0 nm) due to the increased translations and rotations of water compared to water molecules in bulk water.
- Hydrogen bonds between water molecules in the larger (8,8) and (9,9) carbon nanotubes (1.1–1.2 nm) impart favorable enthalpic contributions due to a rigid hydrogen bonding network.
- Large translational entropy of water molecules in the 1.4 nm (10,10) nanotube and larger compared to bulk water induces spontaneous filling.

The splitting of the filling driving force into three domains of pore diameter also represents the structure of water in the nanotube in each case (Pascal et al. 2011). For the smaller pore sizes, the water is restricted to a single file along the pore axis, resulting in a gas-like phase of water molecules. The next largest domain, incorporating the (8,8) and (9,9) carbon nanotubes, is described as an ice-like phase where a slightly increased number of hydrogen bonds per water molecule, as compared to bulk water, restrict the water distribution to a torus perpendicular to the pore axis, as shown in Figure 12.7. As the pore diameter increases further, the structure of water in the nanotube becomes more and more liquid-like. Some layering of the water is still present at the interface with the inner nanotube wall, but this dissipates toward the center of the tube. Although a similar analysis on the driving force of filling in boron nitride and silicon carbide nanotubes has not been conducted, it is assumed that a similar process is at play, although the domains of entropy and enthalpic domination may differ.

12.3.2 Water Fluxes

The first suggestion of the impressive water permeation properties of nanotubes was the seminal MD work of Hummer et al. (2001). It was discovered that water permeated a (6,6) carbon nanotube in burst-like motions, during which water molecules move with very little resistance. This occurred solely from diffusion of water through the carbon nanotube; a force was not used to drive water through the nanotube. The average water flux over the course of the simulation was 17 molecules $tube^{-1}$ ns^{-1}, comparable to the flux of a biological counterpart, the aquaporin-1 channel (Zeidel et al. 1992). Many MD studies exploring the water

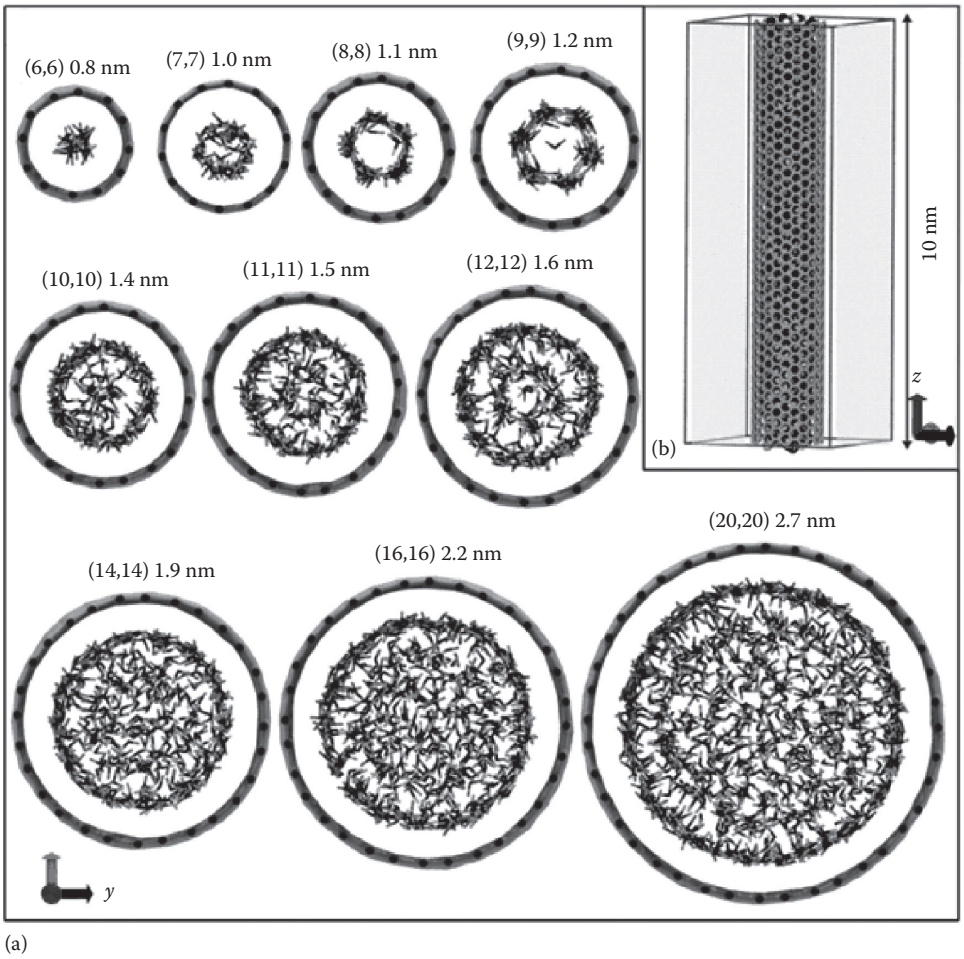

Figure 12.7 The structure of water inside carbon nanotubes of varying diameters. (a) The axial pore distribution looking along the pore axis. (b) A view of the carbon nanotube perpendicular to the pore axis. (Figure is reproduced from Pascal, T.A. et al., *Proc. Natl. Acad. Sci. USA*, 108(29), 11794, 2011.)

permeation properties of various forms of nanotubes followed. A summary of these results are presented in Table 12.1.

It has been suggested that the constant flow observed in nanotubes indicates that there is little to no friction. This is illustrated in Figure 12.8 in which MD studies have shown that the measured axial water velocity profile for carbon nanotubes remains constant to the wall of the nanotube in contrast to the decrease toward the wall in macroscopic flows (Majumder and Corry 2011). In macroscopic models of fluids flowing through a pipe or pore, the velocity of water flow through the pipe is at a minimum at the walls of the pipe and at a maximum at the center of the pipe, similar to the red line in Figure 12.8. Unlike in nanotubes, the friction between water and the pipe causes this slowdown at the walls.

As mentioned, most MD studies investigating water flow through carbon nanotubes assign a zero partial charge to each carbon atom in the nanotube. As a result, there is no electrostatic

TABLE 12.1 WATER FLUXES OF A RANGE OF PRISTINE CARBON (GREEN), BORON NITRIDE (ORANGE), AND SILICON CARBIDE (BLUE) NANOTUBES AS DETERMINED FROM MD SIMULATIONS

Tube Material	Neutral/ Partial Charges	Tube Type	Tube Diameter (nm)	Tube Length (nm)	Driving Force	Magnitude of DF (MPa)	Water Flux (Molecules/ ns/tube)	Reference
Carbon	Neutral	(5,5)	0.66	1.34	HP	208	10.4 ± 0.4	Corry (2008)
Carbon	Neutral	(10,0)	0.78	1.14	Diffusion	—	5.31	Won et al. (2006)
Carbon	Partial charges	(10,0)	0.78	1.14	Diffusion	—	6.69	Won et al. (2006)
Carbon	Neutral	(6,6)	0.81	1.34	Diffusion	—	17	Hummer et al. (2001)
Carbon	Neutral	(6,6)	0.81	1.34	Diffusion	—	5.9 ± 0.8	Zhu and Schulten (2003)
Carbon	Neutral	(6,6)	0.81	1.23	Diffusion	—	4.94	Won et al. (2006)
Carbon	Partial charges	(6,6)	0.81	1.23	Diffusion	—	9.13	Won et al. (2006)
Carbon	Neutral	(6,6)	0.81	2.09	Diffusion	—	15.0	Suk et al. (2008)
Carbon	Neutral	(6,6)	0.81	1.34	OP	—	5.8	Kalra et al. (2003)
Carbon	Neutral	(6,6)	0.81	1.4	HP	208	23.3 ± 0.3	Corry (2008)
Carbon	Neutral	(6,6)	0.81	1.34	HP	15	~8–18	Gong et al. (2008)
Carbon	Neutral	(7,7)	0.93	1.34	HP	208	43.7 ± 0.5	Corry (2008)
Carbon	Neutral	(7,7)	0.95	1.4	HP	100	20.9	Song and Corry (2009)
Carbon	Neutral	(7,7)	0.95	1.4	HP	200	41.3	Song and Corry (2009)
Carbon	Neutral	(8,8)	1.09	1.34	HP	208	81.5 ± 1.2	Corry (2008)
Carbon	Neutral	(8,8)	1.08	1.4	HP	100	39.4	Song and Corry (2009)

(*Continued*)

TABLE 12.1 (*CONTINUED*) WATER FLUXES OF A RANGE OF PRISTINE CARBON (GREEN), BORON NITRIDE (ORANGE), AND SILICON CARBIDE (BLUE) NANOTUBES AS DETERMINED FROM MD SIMULATIONS

Tube Material	Neutral/ Partial Charges	Tube Type	Tube Diameter (nm)	Tube Length (nm)	Driving Force	Magnitude of DF (MPa)	Water Flux (Molecules/ ns/tube)	Reference
Carbon	Neutral	(8,8)	1.08	1.4	HP	200	78.8	Song and Corry (2009)
Carbon	Neutral	(8,8)	1.09	1.3	HP	246	107.8 ± 0.6	Corry (2011)
Carbon	Neutral	(9,9)	1.22	1.4	HP	100	57.4	Song and Corry (2009)
Carbon	Neutral	(9,9)	1.22	1.4	HP	200	110	Song and Corry (2009)
Carbon	Neutral	(50,50)	7	6.1	HP	290	4660 ± 33	Majumder and Corry (2011)
Boron nitride	Partial charges	(5,5)	0.79	1.4	HP	60–612	1.6–10.7	Hilder et al. (2009)
Boron nitride	Neutral	(6,6)	0.83	2.13	Diffusion	—	16.0	Suk et al. (2008)
Boron nitride	Neutral	(6,6)	0.83	2.13	HP	100–500	~12–49	Suk et al. (2008)
Silicon carbide	Partial charges	(5,5)	0.86	3.6	HP	100	17.16	Hilder et al. (2012)
Silicon carbide	Partial charges	(6,6)	1.03	3.6	HP	100	32.33	Hilder et al. (2012)
Silicon carbide	Partial charges	(7,7)	1.2	3.6	HP	100	69.26	Hilder et al. (2012)

Note: HP is hydrostatic pressure and OP is osmotic pressure.

interaction between the nanotube and the water molecules, only van der Waals interactions. The interaction between neutral carbon and water molecules tends to be quite weak. This allows water molecules to adopt particular orientations and hydrogen bonding at the water/nanotube interface, making the surface of the nanotube *slippery* to water molecules (Joseph and Aluru 2008). The near-frictionless flow of water through nanotube implies that the water flux is independent of the length of the tube, which has been confirmed by various MD simulations studies (Kalra et al. 2003, Corry 2008, Nicholls et al. 2012). However, if nonzero partial

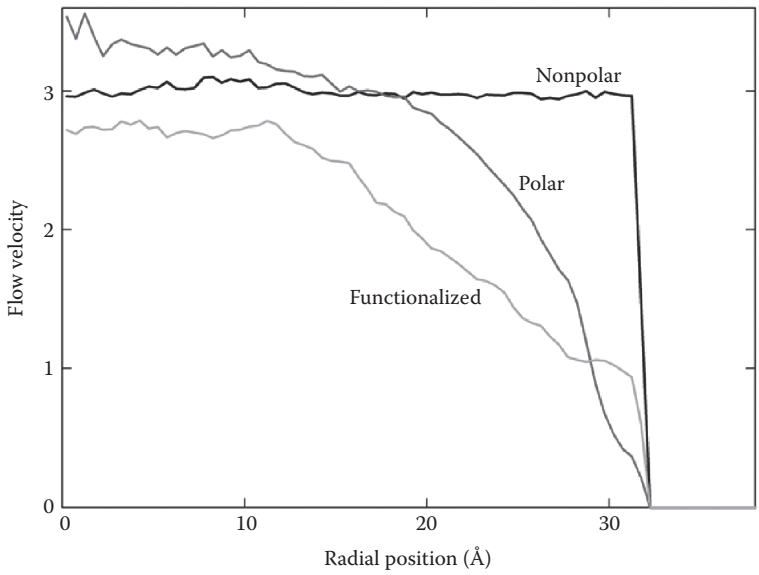

Figure 12.8 The axial velocity profile of water through various carbon nanotubes. Results are shown for a pristine uncharged carbon nanotube (nonpolar), a pristine partially charged carbon nanotube (polar), and a nanotube with bulky negatively charged functional groups attached along the length of the pore (functionalized). The center of the pore is at 0 Å, and the wall of the carbon nanotube is at 35 Å. (From Majumder, M. and Corry, B., Anomalous decline of water transport in covalently modified carbon nanotube membranes, *Chem. Commun.*, 47(27), 7683–7685, 2011. Adapted by permission of The Royal Society of Chemistry.)

charges are assigned to each atom in the carbon nanotube, stronger electrostatic interactions are possible. These interactions slow down the rate at which water can flow across the surface thus creating friction, as can be seen in Figure 12.8 (Majumder and Corry 2011).

Water molecules have been demonstrated to induce charges on carbon nanotube atoms (Lu et al. 2004). Won et al. (2006) determined the charges present in a (6,6) and a (10,0) carbon nanotube using quantum mechanical calculations and implemented these in MD simulations. The partial charges on the carbon atoms near the opening of the nanotubes were found to deviate significantly from zero, while the remainder were approximately zero. In both instances, the addition of these partial charges increased the water fluxes compared with uncharged tubes. Upon inspection of the PMFs in Figure 12.9, it can be seen that the addition of these charges lowers the free energy barrier that a water molecule must overcome to permeate through the pore between 0.32 and 0.56 k_BT. The free energy barrier for a water molecule to enter the pore is lowered due to the increased interactions with the partially charged pore opening. In the carbon nanotubes with zero partial charge on each atom, the transition of water from the bulk to the confined hydrophobic pore incurs a larger free energy penalty.

Due to the heterogeneous constituents of boron nitride and silicon carbide nanotubes, each atom in the nanotube will have a partial charge. Water fluxes in boron nitride tubes are potentially larger than those displayed by comparable diameter carbon nanotubes (Won and Aluru 2007, 2008). The partial charges lower the free energy barrier for water molecules to enter the pore even if there are slightly increased interactions along the length of the pore. If the partial charges of boron nitride and silicon carbide nanotubes are further increased, a decline in the water fluxes is seen (Won and Aluru 2008, Hilder et al. 2009). The electrostatic interactions

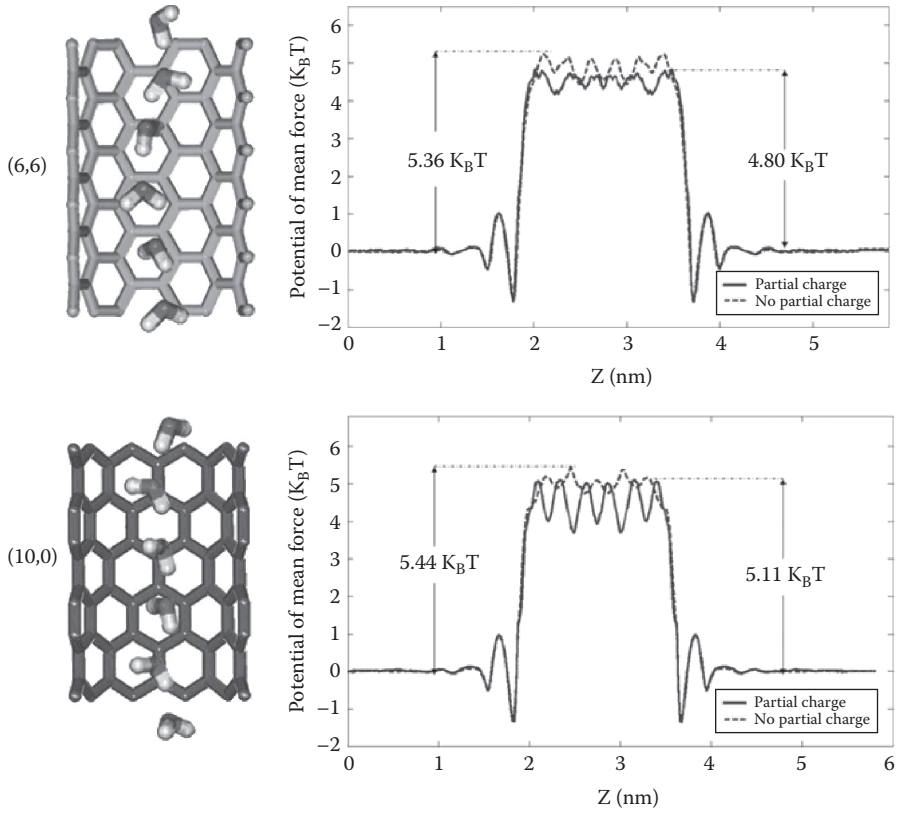

Figure 12.9 The free energy surface for a water molecule to permeate through partially charged (solid line) and uncharged (dashed line) (6,6) and (10,0) carbon nanotubes. (Adapted with permission from Won, C.Y., Joseph, S., and Aluru, N.R., Effect of quantum partial charges on the structure and dynamics of water in single-walled carbon nanotubes, *J. Chem. Phys.*, 125(1), 115701, 2006. Copyright 2006 American Institute of Physics.)

between the water molecules and the nanotube wall become so great with these increased partial charges that the water molecules interact with sections of the nanotube wall for long periods of time, introducing a large of amount of friction to the water flow.

12.3.3 Salt Rejection

Nanotubes have also been studied for their ability to reject salt ions. The experimental work by Fornasiero et al. (2008) demonstrated that 1–2 nm carbon nanotubes are capable of salt rejection. It was determined that salt rejection depends on a number of factors including solution pH and the valency of the ions. These factors indicate that rejection of the ions is occurring via electrostatic interactions between the carbon nanotube pore opening or membrane surface and the ions, rather than steric hindrance at the nanotube opening. Due to the sensitivity of salt rejection to pH, negatively charged carboxylate groups are thought to line the pore entrance of the nanotube. Rejection of 600 mM (roughly the concentration of salt in seawater) KCl solution was found to be 40%–50%, which decreased as this concentration increased. Other potassium salts were tested for salt rejection, demonstrating that salts containing higher valence anions

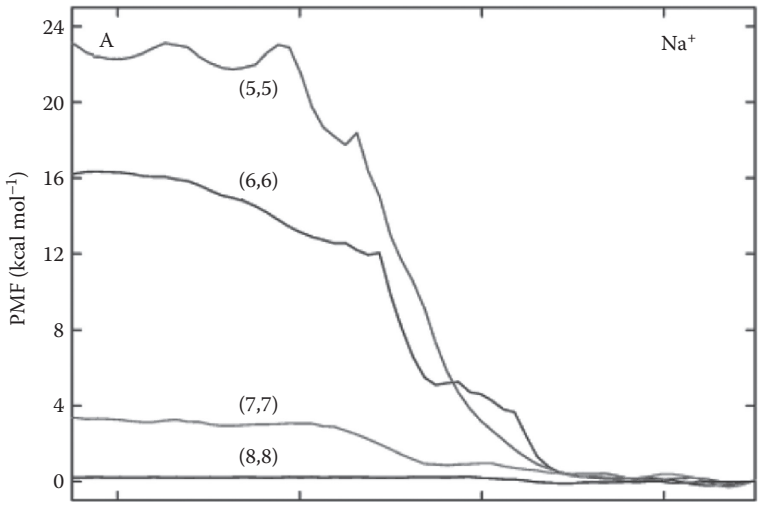

Figure 12.10 The free energy profile of Na^+ permeating through carbon nanotubes of various pore diameters. The left-hand side of the graph is the center of the nanotube and the right-hand side is bulk water. (Reprinted with permission from Corry, B.A., Designing carbon nanotube membranes for efficient water desalination, *J. Phys. Chem. B*, 112(5), 2008, 1427–1434. Copyright 2008 American Chemical Society.)

displayed better rejection for both anions and cations. However, in MD simulations, only NaCl and KCl salts have been modeled so far.

The potential of nanotubes to reject ions while maintaining large water fluxes was first noted in MD simulations by Kalra et al. (2003). Using an osmotic gradient, water molecules were shown to flow through a membrane composed of (6,6) carbon nanotubes from the freshwater reservoir to the saltwater reservoir, with Na^+ and Cl^- ions never flowing in the opposite direction. Further investigations identified a large free energy barrier for Na^+ ions to permeate across (6,6), 0.81 nm diameter carbon nanotubes but a relatively small barrier for the larger 1.4 nm (10,10) nanotubes (Peter and Hummer 2005). This indicated that there may be a critical pore diameter below which the 95% salt rejection required for desalination could be achieved. A subsequent investigation quantitatively determined the salt rejection of (5,5), (6,6), (7,7), and (8,8) (0.66, 0.81, 0.93, 1.09 nm diameter, respectively) carbon nanotubes under a hydrostatic pressure of 208 MPa to be 100%, 100%, 95%, and 58% (Corry 2008). Displayed in Figure 12.10 is the PMF of a Na^+ ion passing through these tubes, (Corry 2008) showing the large energy barrier for the narrow (5,5) carbon nanotube and the very small barrier for the wider (8,8). These results indicate that fewer than 1 in 100 nanotubes in a reverse osmosis membrane could have a diameter larger than 0.93 nm tube to maintain an overall 95% salt rejection. This is an important result to guide the manufacturing of carbon nanotube membranes as their fabrication produces a wide distribution of pore diameters, rather than a single diameter.

The partial charges of water molecules are attracted to the charge of the ion resulting in the formation of a shell of water around the ion, called the solvation shell. The number of water molecules in this shell is the coordination number for that ion. For an ion to enter the narrower tubes, some of the water molecules in the solvation shell must be removed, so that the ion may fit. Removing these water molecules incurs an energetic penalty and so creates the energy barriers observed in Figure 12.10. For instance, as illustrated in Figure 12.11, a Na^+ ion has a coordination number of about 6 in bulk water, but this must reduce to 2 inside a (5,5), 0.66 nm carbon

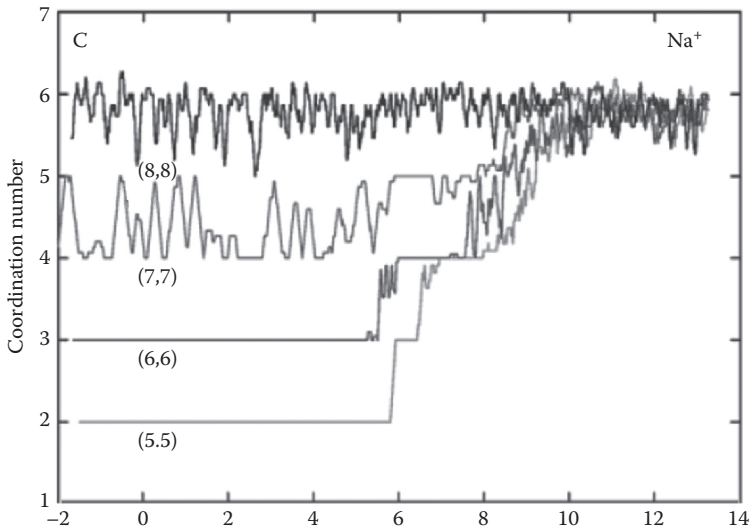

Figure 12.11 The coordination number of a Na^+ ion as it moves from carbon nanotubes of various diameter pores (left-hand side of graph) to bulk water (right-hand side of graph). (Reprinted with permission from Corry, B.A., Designing carbon nanotube membranes for efficient water desalination, *J. Phys. Chem. B*, 112(5), 2008, 1427–1434. Copyright 2008 American Chemical Society.)

nanotube (Corry 2008). As the pore diameter increases, fewer water molecules are required to be removed from the solvation shell for the ion to move through the nanotube. At a diameter of 1.09 nm (a (8,8) carbon nanotube), the coordination number inside the tube is similar to that in bulk water.

Pristine boron nitride nanotubes also have the ability to reject salt. One MD study used hydrostatic pressure to force a NaCl solution through a single boron nitride nanotube embedded in a silicon nitride membrane (Hilder et al. 2009). The 0.69 nm diameter, (5,5) boron nitride nanotubes completely reject both Na^+ and Cl^- ions. The large energy barrier for ion permeation through this nanotube (determined by calculating the PMF of each ion) was found to result from the removal of numerous water molecules from the coordination shell of each ion. This large dehydration barrier remains for Cl^- permeation through 0.83 nm diameter, (6,6) boron nitride nanotubes, but completely disappears for Na^+. It is speculated that this results from the unique electrostatic interactions present in the boron nitride nanotubes due to the partial charges on the boron and nitrogen atoms in combination with the water structure inside the nanotube. A similar situation is found in the 0.97 nm diameter, (7,7) boron nitride nanotubes. In stark contrast, the salt rejection properties are reversed in the 1.1 nm (8,8) nanotubes; Na^+ is completely rejected, while Cl^- is able to pass. The structure of the water molecules in this nanotube is highly ordered and has been described as ice-like, similar to the water structure in the (8,8) and (9,9) carbon nanotubes. The presence of Cl^- causes minimal deviation of water molecules from this structure, while Na^+ causes a large reordering of water molecules, causing a large free energy barrier. This has also been recently observed in carbon nanotubes (He et al. 2013).

The ion rejection properties in (5,5), (6,6), and (7,7) silicon carbide nanotubes have also been determined through MD simulations (Hilder et al. 2012). The 0.86 nm diameter (5,5) nanotube completely rejected both Na^+ and Cl^-, much like its boron nitride counterpart. However, unlike

boron nitride nanotubes, the rejection properties of Na^+ and Cl^- in the 1.0 nm (6,6) and 1.2 nm (7,7) silicon carbide nanotubes are reversed; Cl^- is able to permeate the pores, while Na^+ is rejected. This reversal is due predominantly to the large radial buckling present in the smaller-diameter silicon carbide nanotube (Alam and Ray 2007, 2008). The positive partially charged silicon atoms are closer to the center of the pore than the negatively partially charged carbon atoms. Due to simple electrostatic interactions, this makes the pore much more hospitable to the negatively charged Cl^- and inhospitable to the positively charged Na^+.

The mechanism of ion rejection in MD studies of pristine nanotubes differs from that in experimental investigations of nanotubes. The former focuses on narrow nanotubes, usually with pore diameters about 1 nm or less, whereas the latter investigates nanotubes with pores wider than 1 nm. Ions need to dehydrate to enter narrow tubes; a size exclusion mechanism is operating on hydrated and bare ions. Ion rejection in wider nanotubes is caused by electrostatic interactions between ions and functional groups at the nanotube pore opening.

12.3.4 Functionalization

During the manufacturing of membranes containing aligned nanotubes, the matrix in which the nanotubes are embedded must be etched to expose the tubes. Further etching removes the nanotube cap creating an open pore through the matrix. The etching process has been found to introduce chemical species that covalently bond to carbon atoms at the pore openings of nanotubes, known as functionalization (Majumder et al. 2005, Yang et al. 2005, Li et al. 2007). Typical functional groups include carboxylic (–COOH), hydroxyl (–OH), and carbonyl (C=O) groups. These functional groups can alter the water flux and ion rejection properties of nanotubes. The additional electrostatic interactions between these functional groups and water/ions are the main cause of these alterations, with steric and hydrodynamic effects playing only a small role (Fornasiero et al. 2008).

A detailed study by Corry determined how many different types of functionalizations can affect the properties of nanotubes (Corry 2011). In this investigation, 1.1 nm (8,8) carbon nanotubes were functionalized with varying numbers (either 2, 4, or 8) of COO^-, NH_3^+, OH (as shown in Figure 12.12), and $CONH_2$ functional groups, as well as a mixtures of NH_4^+ and COO^-, at the upstream pore opening. One or three of these functionalized carbon nanotubes were placed in an array with pristine carbon nanotubes (see Figure 12.5d as an example). Three configurations obtained 100% rejection of Na^+ and Cl^- ions, greater than the required 95%: 8 COO^-, $4NH_4^+$, and $3 \times 4NH_4^+$. The $3 \times 2NH_4^+$ obtained Na^+ and Cl^- rejection of 94% and 92%, just below the required 95%. Each of these improved on the rejection in pristine (8,8) nanotubes, which displayed Na^+ and Cl^- rejection of 28% and 86%, respectively. However, the most marked difference between the pristine and functionalized carbon nanotubes was the reduction in the water flux for all tested functionalized nanotubes, ranging from 67% to 13% of the pristine carbon nanotube flux. The three functionalized nanotubes obtaining sufficient Na^+ and Cl^- rejection displayed some of the lowest water fluxes with 13%, 24%, and 25% of the pristine fluxes for $8COO^-$, $4NH_4^+$, and $3 \times 4NH_4^+$, respectively. However, these water fluxes still equate to 3, 4.8, and 5.3 times larger than a common commercially used RO membrane SW30HR-380 assuming a packing density of carbon nanotubes in a matrix that has been achieved experimentally.

The reduction in water fluxes is due to the increased electrostatic interactions between water molecules and the functional groups, as well as steric blockages of the pore entrance. The strong electrostatic interactions between the water molecules and the functional groups increase the time that a water molecule spends at the pore entrance, slowing down the passage of following

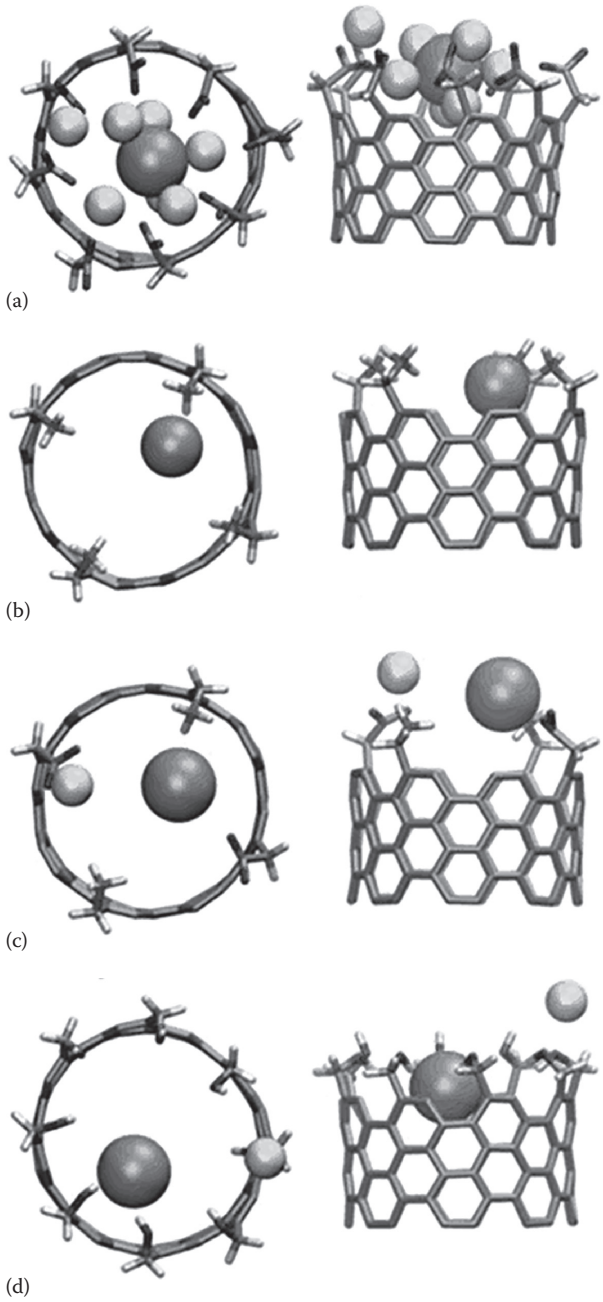

Figure 12.12 Top (left) and side (right) views of the position of ions near the pore opening of functionalized carbon nanotubes. Na^+ is represented by small spheres and Cl^- by large spheres. The carbon nanotubes depicted here are functionalized by (a) $8COO^-$, (b) $4NH_4^+$, (c) $2COO^-$, and $2NH_4^+$, and (d) 8OH. (From Corry, B., Water and ion transport through functionalised carbon nanotubes: Implications for desalination technology, *Energy Environ. Sci.*, 4(3), 751–759, 2011. Reproduced by permission of The Royal Society of Chemistry.)

water molecules. Steric blockages can be caused by ions binding strongly to the functional groups or by the functional groups themselves; both these mechanisms reduce the area through which water can enter the nanotube pore.

The addition of functional groups at the pores' entrance can also affect the salt rejection of the nanotube. The situation is complicated by factors such as the pore diameter and the flexibility of the functional groups. For example, Cl^- rejection will increase if narrow nanotubes are functionalized with COO^- groups due to electrostatic repulsion. However, in wider nanotubes, Na^+ will aggregate around these COO^- groups, shielding the negative charge of the functional groups, allowing Cl^- to pass through the nanotube. This situation is illustrated in Figure 12.12a.

The mechanism of water retardation proposed by Corry is supported by further investigations by Hughes et al. (Hughes et al. 2012). In this study, arrays of aligned carbon nanotubes were functionalized with a range and combination of chemical moieties. It was found that electrostatic interactions between the water molecules and functional groups reduce water diffusion through the nanotube when compared to a pristine nanotube. The effect was greatest when the nanotube was functionalized with carboxylic acid (COOH) or carboxylate (COO^-) groups. Ion rejection is increased when the nanotubes are functionalized with these groups.

12.3.5 Ion Selectivity

Ion selectivity can be defined as a significant difference in the ability of a pore to pass/reject two ion types. This ability is very important in various biological processes; the selection between anions and cations is important for the regulation of blood pressure and organelle acidification, while the selection between Na^+ and K^+ is important for nerve conduction and maintaining electrochemical gradients across cells. Many proteins have developed the ability to discern between these ions, making these processes possible. One particular class of these proteins, called ion channels, are able to distinguish between ion types at near diffusion-limited rates. Nanotubes have the ability to mimic and replicate these properties for use in a range of applications, including ultrasensitive ion detection and antimicrobial agents.

The free energy barriers for ions to permeate a pristine nanotube can be different for different ion types due to the differences in dehydration energy for each ion type, making it more likely for some ions to pass than others. Ion selectivity has been investigated between Na^+, K^+, and Cl^- in pristine (5,5), (6,6), (7,7), (8,8), and (9,9) carbon nanotubes using MD simulations (Song and Corry 2009). For Na^+/K^+ selectivity, the PMF for each ion permeating each nanotube demonstrated that the free energy barrier was larger for K^+ in (5,5) and (6,6) carbon nanotubes, for Na^+ in (7,7) and (8,8) nanotubes, and roughly equal in (9,9) nanotubes. Na^+ has on average fewer (~6), but more tightly bound, water molecules in its coordination shell in bulk, whereas K^+ has more (~7), but less strongly bound water molecules. In the narrower (5,5) and (6,6) nanotubes, many water molecules are stripped from each ion, which is more energetically costly for Na^+ than K^+ as they are more tightly bound to Na^+. In the wider (7,7) and (8,8) carbon nanotubes, Na^+ is able to permeate with close to its full complement of water molecules, while some must still be stripped from K^+ for it to permeate. In the (9,9) carbon nanotubes, both ions are to pass with their full complement of water molecules, so there is little difference in their energy barriers. Similar principles have been shown for selection between anions in simplified narrow pores (Richards et al. 2012, 2012b).

Ion selectivity has been demonstrated in a range of other nanotube structures. For example, (9,9) carbon nanotubes functionalized with carbonyl groups at the pore openings are selective for Cl^- over Na^+ (Hilder et al. 2010). These nanotubes display similar conductance properties as

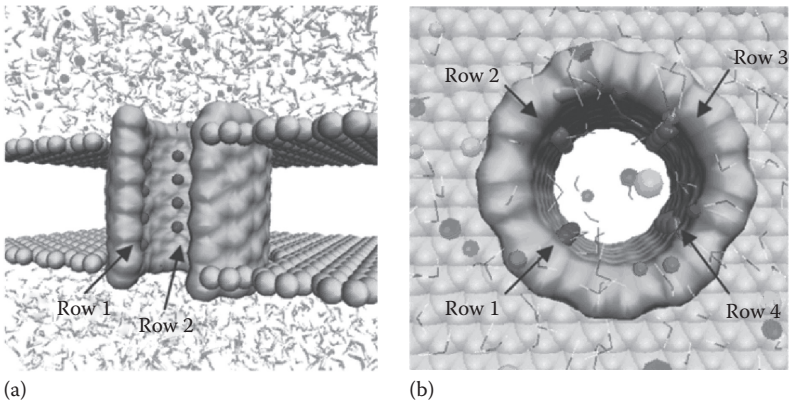

Figure 12.13 (a) Side and (b) top views of a (9,9) carbon nanotube functionalized with carbonyl (C=O) groups. The offset form is presented in this figure. (Reprinted with permission from Gong, X., Li, J., Xu, K., Wang, J., and Yang, H., A controllable molecular sieve for Na^+ and K^+ ions, *J. Am. Chem. Soc.*, 132(6), 2010, 1873–1877. Copyright 2010 American Chemical Society.)

biological Cl^--selective ion channels, such as ClC channels and GABA receptors. In addition, (6,6) and (7,7) boron nitride nanotubes are selective for Na^+ over Cl^- (Hilder et al. 2009a), while (10,10) boron nitride nanotubes are selective for Cl^- over K^+, the opposite of the selectivity found in (10,10) carbon nanotubes (Won and Aluru 2009). Differences in water structure, buckling, and ion dehydration energies produce different energy barriers for different ions to permeate the pore, resulting in selectivity. Pristine (6,6) and (7,7) silicon carbide nanotubes have an intrinsic selectivity for Cl^- over Na^+ (Hilder et al. 2012). The energy barrier for Na^+ permeation is much larger than Cl^- due to its water molecules being more strongly bound than Cl^-.

The interior of pores have been targeted as sites of functionalization, rather than the pore openings, in an attempt to mimic biological ion-selective structures (Gong et al. 2010). MD simulations of a (9,9) carbon nanotube functionalized with carbonyl oxygens, as shown in Figure 12.13, determined the selectivity between Na^+ and K^+. Three different configurations of carbonyl groups were studied, each producing marked differences in selectivity. The configuration mimicking the selectivity filter of a potassium channel (four sets of four carbonyl oxygens arranged in four rings) resulted in a Na^+-selective nanotube. When half of the carbonyl oxygen atoms were offset from the ring structure to a spiral structure (Figure 12.13a), the nanotube was nonselective. When two rows of carbonyl oxygen are removed from this structure, the nanotube exhibited K^+ selectivity. These results are surprising as the K^+ channel mimic selected for Na^+. It is difficult, if not impossible, to predict *a priori* the selectivity of functionalized nanotubes, given the number of factors involved in determining selectivity.

12.4 PRACTICAL FEASIBILITY AND CONCLUSIONS

The water and ion permeation properties of nanotubes make them ideal for use in many types of applications. Seawater desalination is a prime application for nanotube-based reverse osmosis membranes. MD simulations have demonstrated that some nanotubes have greatly increased water fluxes compared to commercially available membranes, while being able to maintain the

necessary 95% salt rejection that is required for potable water. However, there are two issues that may limit the implementation of this technology.

A very narrow distribution of nanotube pore diameters is required in order to maintain the necessary salt rejection, a range of only 0.66–0.93 nm for unfunctionalized carbon nanotubes. Holt et al. (2006) and Fornasiero et al. (2008) have fabricated carbon nanotubes in membranes in the diameter range of 1–2 nm. Although smaller-diameter nanotubes have been fabricated—down to 0.4 nm (Guan 2008)—it is unclear how these nanotubes could be grown or placed in an aligned manner into a membrane matrix, while maintaining such a small range of pore sizes.

The second issue is the implementation of the nanotube-based reverse osmosis membranes into desalination facilities. Modern facilities typically operate at a recovery rate of 50%: half of the intake saltwater is desalinated, while the other half doubles in salt concentration. These facilities operate at a pressure a few percent above the osmotic pressure of this hypersaline solution. Most of the energy put into the reverse osmosis process is used to overcome this osmotic pressure, not to work against the friction encountered by water permeating through the membrane. Nanotube-based reverse osmosis membranes may save up to about 1% of energy used in this process, but some researchers argue that effort and money are better spent improving other processes in the desalination facility (Elimelech and Phillip 2011). It could be argued that nanotube-based membranes could save on capital costs by requiring less surface area than currently implemented membranes, to achieve the same potable water fluxes. However, for the foreseeable future, the cost of nanotube-based membranes will far outweigh the cost of purchasing and installing more traditional membrane modules. A possible advantage of having a high-flux nanotube membrane would lie in reduced size of the desalination plant, which may find specialized applications in places where size and weight are limited, for example, space missions.

Nanotube-based membranes may still prove to be more resistant to fouling, a common problem in currently used membranes. A number of organic and inorganic species are able to physically and chemically occlude pores, and therefore membranes must be regularly cleaned. Carbon nanotubes have been demonstrated to be able to be readily functionalized; perhaps the more chemically inert boron nitride and silicon nitride nanotubes will be more resistant to fouling. More research is required to determine the ability of these nanotubes to resist fouling. MD is not able to simulate chemical reactions taking place during chemical fouling of the membrane. There are other computational techniques that are available to study this such as quantum mechanical and hybrid quantum mechanical/molecular dynamic techniques. However, fouling in the form of physical blockage could potentially be modeled by MD for small fouling species.

The recycling of wastewater is becoming more popular as traditional water sources become scarcer. Filtration techniques employed by water treatment facilities allow some potentially harmful molecules such as endocrine-disrupting chemicals to pass through (Johnson and Sumpter 2001). In addition, it has been determined that traditional nanofiltration membranes allow the passage of hormones such as testosterone and progesterone (Ngheim et al. 2004). The selectivity properties of nanotube-based membranes make them ideal candidates as filtration membranes. The more rigid structure of nanotubes than polymers can allow for high levels of selectivity, which may be useful for filtering of these species.

MD is a computer simulation technique that provides a powerful tool to investigate transport in nanotubes. Nanotubes possess some very interesting properties, such as the high water throughputs and salt rejection. Water traverses through nanotube pores with almost frictionless flow, a unique property of nanotubes. Coupled with the salt rejection properties, this makes

many types of nanotubes ideal for high-throughput saltwater desalination. There are many other applications of selective nanotube pores that are not discussed in this chapter, for example, biosensors and nanofluid devices, and we anticipate that they will find uses in a range of unexpected areas in the future.

REFERENCES

Alam, K. M. and Ray, A. K., A hybrid density functional study of Zigzag SiC nanotubes. *Nanotechnology* 18(49) (2007):495706.

Alam, K. M. and Ray, A. K., Hybrid density functional study of armchair SiC nanotubes. *Phys. Rev. B.*, 77(3) (2008):035436.

Alexiadis, A. and Kassinos, S., Molecular simulation of water in carbon nanotubes. *Chem. Rev.* 108(12) (2008):5014–5034.

Beckstein, O. and Samsom, M. S. P., The influence of geometry, surface character, and flexibility on the permeation of ions and water through biological pores. *Phys. Biol.* 1(1) (2004):42–52.

Corry, B., An energy-efficient gating mechanism in the acetylcholine receptor channel suggested by molecular and Brownian dynamics. *Biophys. J.* 90(3) (2006):799–810.

Corry, B., Water and ion transport through functionalised carbon nanotubes: Implications for desalination technology. *Energy Environ. Sci.* 4(3) (2011):751–759.

Corry, B. A., Designing carbon nanotube membranes for efficient water desalination. *J. Phys. Chem. B* 112(5) (2008):1427–1434.

Dzubiella, J. and Hansen, J. -P., Electric-field-controlled water permeation of a hydrophobic nanopore. *J. Chem. Phys.* 122(23) (2005):234706.

Elimelech, M. and Phillip W. A., The future of seawater desalination: Energy, technology, and the environment. *Science* 333(6043) (2011):712–717.

Fornasiero, F., Park, H. G., Holt, J. K. et al., Ion exclusion by sub-2-nm carbon nanotube pores. *Proc. Natl. Acad. Sci. U.S.A.* 105 (2008):17250–17255.

Gong, X., Li, J., Xu, K., Wang, J., and Yang, H., A controllable molecular sieve for Na^+ and K^+ ions. *J. Am. Chem. Soc.* 132(6) (2010):1873–1877.

Gong, X., Li, J., Zhang, H. et al., Enhancement of water permeation across a nanochannel by the structure outside the channel. *Phys. Rev. Lett.* 101(25) (2008):257801.

Guan, L., Suenaga, K., and Iijima, S., Smallest carbon nanotube assigned with atomic resolution accuracy. *Nano Lett.* 8(2)(2007):459–462.

He, Z., Zhou, J., Lu, X., and Corry, B., Ice-like water structure in carbon nanotube (8,8) induces cationic hydration enhancement. *J. Phys. Chem. C* 117(21) (2013):11412–11420.

Hilder, T. A., Gordon. D., and Chung, S. -H., Salt rejection and water transport through boron nitride nanotubes. *Small* 5(19) (2009):2183–2190.

Hilder, T. A., Gordon, D. and Chung S. -H., Boron nitride nanotubes selectively permeable to cations or anions. *Small* 5(24) (2009a):2870–2875.

Hilder, T. A., Gordon, D., and Chung, S. -H., Synthetic chloride-selective carbon nanotubes examined by using molecular and stochastic dynamics. *Biophys. J.* 99(6) (2010):1734–1742.

Hilder, T. A., Gordon, D., and Chung, S. -H., Computational modeling of transport in synthetic nanotubes. *Nanomedicine-UK* 7(6) (2011):702–709.

Hilder, T. A., Yang, R., Gordon, D., Rendell, A. P., and Chung, S. -H., Silicon carbide nanotube as a chloride-selective channel. *J. Phys. Chem. C* 116(7) (2012):4465–4470.

Hinds, B. J., Chopra, N., Rantell, T., Andrews, R., Gavalas, V., and Bachas, L. G., Aligned multiwalled carbon nanotube membranes. *Science* 303(5654) (2004):62–65.

Holt, J. K., Park, H. G., Wang, Y. et al., Fast mass transport through Sub-2-nanometer carbon nanotubes. *Science* 312(5776) (2006):1034–1037.

Hughes, Z. E., Shearer, C. J., Shapter, J., and Gale, J. D., Simulation of water transport through functionalized Single-Walled Carbon Nanotubes (SWCNTs). *J. Phys. Chem. C* 116(47) (2012):24943–24953.

Hummer, G., Rasaiah, J. C., and Noworyta, J. P., Water conduction through the hydrophobic channel of a carbon nanotube. *Nature* 414 (2001):188–190.

Humphrey, W., Dalke, A., and Schulten, K., VMD: Visual molecular dynamics. *J. Mol. Graphics*, 14(1) (1996):33–38.

Johnson, A. C. and Sumpter, J. P., Removal of endocrine-disrupting chemicals in activated sludge treatment works. *Environ. Sci. Technol.* 35(24) (2001):4697–4703.

Joseph, S. and Aluru, N. R., Why are carbon nanotubes fast transporters of water? *Nano Lett.* 8(2) (2008):452–458.

Kalra, A., Garde, S., and Hummer, G., Osmotic water transport through carbon nanotube membranes. *Proc. Natl. Acad. Sci. U.S.A.* 100(18) (2003):10175–10180.

Kumar, S., Bouzida, D., Swendsen, R. H., Kollman, P. A., and Rosenberg, J. M., The weighted histogram analysis method for free-energy calculations on biomolecules. I. The method. *J. Comput. Chem.* 13(8) (1992):1011–1021.

Li, P. H., Lim, X., Zhu, Y. et al., Tailoring wettability change on aligned and patterned carbon nanotube films for selective assembly. *J. Phys. Chem. B* 111(7) (2007):1672–1678.

Lu, D., Li, Y., Rotkin, S. V., Ravaioli, U., and Schulten, K., Finite-size effect and wall polarization in a carbon nanotube channel. *Nano Lett.* 4(12) (2004):2383–2387.

MacKerell, A. D. Jr., Bashford, D., Bellott, M. et al., All-atom empirical potential for molecular modeling and dynamics studies of proteins. *J. Phys. Chem. B* 102(18) (1998):3586–3616.

Maiti, A. Carbon nanotubes: Bandgap engineering with strain. *Nat. Mater*. 2 (2003):440–442.

Majumder, M., Chopra, N., Andrews, R., and Hinds, B. J., Enhanced flow in carbon nanotubes. *Nature* 438 (2005):44.

Majumder, M. and Corry, B., Anomalous decline of water transport in covalently modified carbon nanotube membranes. *Chem. Commun.* 47(27) (2011):7683–7685.

Nghiem, L. D., Schäfer, A. I., and Elimelech, M., Removal of natural hormones by nanofiltration membranes: Measurement, modeling, and mechanisms. *Environ. Sci. Technol.* 38(6) (2004):1888–1896.

Nicholls, W. D., Borg, M. K., Lockerby, D. A., and Reese, J. M., Water transport through (7,7) carbon nanotubes of different lengths using molecular dynamics. *Microfluid Nanofluid* 12(1–4) (2012):257–264.

Pascal, T. A., Goddard, W. A., and Jung, Y., Entropy and the driving force for the filling of carbon nanotubes with water. *Proc. Natl. Acad. Sci. U.S.A.* 108(29) (2011):11794–11798.

Peter, C. and Hummer, G., Ion transport through membrane-spanning nanopores studied by molecular dynamics simulations and continuum electrostatic calculations. *Biophys. J.* 89(4) (2005):2222–2234.

Richards, L. A., Schäfer, A. I., Richards, B. S., and Corry, B., The importance of dehydration in determining ion transport in narrow pores. *Small* 8(11) (2012):1701–1709.

Richards, L. A., Schäfer, A. I., Richards, B. S. and Corry, B., Quantifying barriers to monovalent anion transport in narrow non-polar pores. *Phys. Chem. Chem. Phys.* 14(33) (2012b):11633–11638.

Salomon-Ferrer, R., Case, D. A., and Walker, R. C. An overview of the amber biomolecular simulation package. *WIREs Comput. Mol. Sci.* 3(2) (2013):198–210.

Scott, W. R. P., Hünenberger, P. H., Tironi, I. G. et al., The GROMOS biomolecular simulation program package. *J. Phys. Chem. A* 103(19) (1999):3596–3607.

Song, C. and Corry, B., Intrinsic ion selectivity of narrow hydrophobic pores. *J. Phys. Chem. B* 113(21) (2009):7642–7649.

Su, J. and Guo, H., Effects of nanochannel dimension on the transport of water molecules. *J. Phys. Chem. B* 116(20) (2012):5925–5932.

Suk, M. E., Raghunathan, A. V., and Aluru, N. R., Fast reverse osmosis using boron nitride and carbon nanotubes. *Appl. Phys. Lett.* 92(13) (2008):133120.

Taghavi, F., Javadian, S., and Hashemianzadeh, S. M., Molecular dynamics simulations of single-walled silicon carbide nanotubes immersed in water. *J. Mol. Graph. Model.* 44 (2013):33–43.

Torrie, G. and Valleau, J., Monte Carlo free energy estimates using non-Boltzmann sampling: Application to the sub-critical lennard-jones fluid. *J. Chem. Phys. Lett.* 28(4) (1974):578–581.

Valavala, R., Sohn, J., Han, J., Her, N., and Yoon, Y., Pretreatment in reverse osmosis seawater desalination: A short review. *Environ. Eng. Res.* 16(4) (2011):205–212.

Won, C. Y., Joseph, S., and Aluru, N. R., Effect of quantum partial charges on the structure and dynamics of water in single-walled carbon nanotubes. *J. Chem. Phys.* 125(1) (2006):115701.

Won, C. Y. and Aluru, N. R., Water permeation through a subnanometer boron nitride nanotube. *J. Am. Chem. Soc.* 129(10) (2007):2748–2749.

Won, C. Y. and Aluru, N. R., Structure and dynamics of water confined in a boron nitride nanotube. *J. Phys. Chem. C* 112(6) (2008):1812–1818.

Won, C. Y. and Aluru, N. R., A chloride ion-selective boron nitride nanotube. *Chem. Phys. Lett.* 478(4–6) (2009):185–190.

Yang, D. -Q., Rochette, J. -F., and Sacher, E., Controlled chemical functionalization of multiwalled carbon nanotubes by kiloelectronvolt argon ion treatment and air exposure. *Langmuir* 21(18) (2005):8539–8545.

Yang, R., Hilder, T. A., Chung, S. -H., and Rendell, A., First-principles study of water confined in single-walled silicon carbide nanotubes. *J. Phys. Chem. C* 115(35) (2011):17255–17264.

Zeidel, M. L., Ambudker, S. V., Smith, B. L., and Agre, P., Reconstitution of functional water channels in liposomes containing purified red cell CHIP28 protein. *Biochemistry* 31(33) (1992):7436–7440.

Zhu, F. and Schulten, K., Water and proton conduction through carbon nanotubes as models for biological channels. *Biophys. J.* 85(1) (2003):236–244.

Zhu, F., Tajkhorshid, E., and Schulten, K., Pressure-induced water transport in membrane channels studied by molecular dynamics. *Biophys. J.* 83(1) (2002):154–160.

Zhu, F., Tajkhorshid, E., and Schulten, K. Theory and simulation of water permeation in aquaporin-1. *Biophys. J.* 86(1) (2004):50–57.